

LH WAVE ABSORPTION BY MODE CONVERSION  
NEAR ION CYCLOTRON HARMONICS\*

K. Ko, A. Bers, and V. Fuchs\*\*

PFC/RR-81-8

February 1981

\* To appear in Proceedings of the 4th Topical Conference on RF Heating of Plasma, University of Texas at Austin, Feb. 1981.

\*\* IREQ, Varennes, Quebec, JOL 2P0

# LH WAVE ABSORPTION BY MODE CONVERSION NEAR ION CYCLOTRON HARMONICS\*

K. Ko, A. Bers, M.I.T. Plasma Fusion Center, Cambridge, MA 02139

V. Fuchs, IREQ, Varennes, Quebec, J0L2P0

Numerical studies of the dispersion relation near the lower-hybrid frequency in an inhomogeneous plasma ( $\nabla n$ ,  $\nabla T$ ,  $\nabla B$ ) show that portions of an incident lower-hybrid wave spectrum undergo successive but partial mode conversions to warm-plasma waves in the presence of ion cyclotron harmonics. Wave absorption beyond the first mode conversion occurs near an ion cyclotron harmonic where ion Landau damping is enhanced. A second-order dispersion relation numerically in good agreement with the full dispersion relation in the mode conversion region is derived using the condition  $\partial D/\partial k = 0$ . The mode conversion efficiency at each confluence is evaluated by solving the corresponding differential equation.

Linear mode conversion of lower hybrid waves in a tokamak plasma with a nonuniform magnetic field is considered. For  $\omega_{ci} \ll \omega \ll \omega_{ce}$  and  $\lambda_i \gg 1$ , the simplified form of the kinetic electrostatic dispersion relation is [1]

$$D_E = k_x^2 + k_z^2 + 2 \frac{\omega_{pe}^2}{V_{Te}^2} [1 + e^{-\lambda_e} I_0(\lambda_e) \zeta_e Z(\zeta_e)] + 2 \frac{\omega_{pi}^2}{V_{Ti}^2} [1 + \zeta_i(Z(\zeta_i) - i\sqrt{\pi}e^{-\zeta_i^2}) + \beta] = 0 \quad (1)$$

where  $\lambda_{i,e} = \frac{k_x^2 V_{Ti,e}^2}{2\omega_{ci,e}^2}$ ,  $\zeta_{i,e} = \frac{\omega}{k_{x,z} V_{Ti,e}}$  and  $\beta = \frac{1}{\sqrt{\pi}} \frac{\omega_{ci}}{k_z V_{Ti}} \sum_{n=-\infty}^{\infty} Z\left(\frac{\omega - n\omega_{ci}}{k_z V_{Ti}}\right) \zeta_i e^{-\zeta_i^2}$ .

$Z$  is the plasma dispersion function and  $I_0$  is the modified Bessel function. Previous lower hybrid mode conversion studies have further taken  $\lambda_e \ll 1$  (magnetized electrons),  $\beta = 0$  (straight-line ion-orbits), and  $\zeta_i \gg 1$  to arrive at the familiar warm plasma dispersion relation [2-6]. Efforts have been made to include damping near the ion cyclotron harmonics as a perturbation by replacing  $k_x$  by  $k_o$  in  $\beta$  where  $k_o$  satisfies the warm plasma dispersion relation. In a typical tokamak, an incoming lower hybrid wave encounters a series of cyclotron harmonics as it travels into the plasma bulk.

Numerical evaluations of the exact dispersion relation  $D_E$  for Alcator-A parameters and profiles ( $\nabla n$ ,  $\nabla T$ ,  $\nabla B$ ), show that while the magnetized electrons approximation is valid, it is necessary to retain the full ion dynamics in order to accurately describe the mode conversion process in the presence of ion cyclotron harmonics [7]. This is due to the fact that  $\zeta_i$  is not sufficiently large for  $Z(\zeta_i)$  to be asymptotically expanded and for the  $\beta$  term to be neglected or be treated perturbatively. The contribution from the ion cyclotron harmonics has two effects on mode conversion. The imaginary part introduces dissipation near the cyclotron harmonics in the form of enhanced ion Landau damping. The real part contributes in between the harmonics thereby effectively shifting the mode conversion locations.

The effect of the ion cyclotron harmonics on mode conversion is qualitatively illustrated by the dispersion curves in Fig. 1 which shows the lower hybrid and the warm plasma branches in the region of interest. A more

\* Work supported by U.S. DOE Contract DE-AC02-78ET-51013.

quantitative measure of the effect is shown in Fig. 3 which gives the confluence points for the lower hybrid and warm plasma branches for a range of  $n_z$ 's ( $n_z = k_z c / \omega$ ) keeping full ion dynamics. These are solutions to the coupled system [8]

$$D_E(k_x, \xi) = 0 \quad (2)$$

$$\frac{\partial D_E}{\partial k_x}(k_x, \xi) = 0 \quad (3)$$

with  $k_x = k_r + ik_i$ ,  $\xi = x + iy$ . Eqs.(2) and (3) define a wave confluence by requiring that the wave condition and the zero group velocity condition be satisfied simultaneously. It is relatively easy to show that without the ion cyclotron harmonics, confluence points occur in pairs, as a result of the parabolic density inhomogeneity. Except for a small range of low  $n_z$  values whose confluence points lie along the imaginary axis or occur close together on the real axis, the major portion of the incident lower hybrid wave spectrum is totally reflected i.e. mode converted. Taking the cyclotron harmonics into account, there is a significant change in the wave energy flow picture with the appearance of new confluence points. In Fig.3 only the confluence points of relevance to the incident lower hybrid wave are shown (..... represents the first confluence point that the incident lower hybrid wave encounters while ..... signifies the second confluence point. In all cases wave propagation is from right to left where  $x = 0$  is the center of the plasma and  $a$  is the minor radius). It is seen that the confluence points are now confined to regions between the harmonics, becoming more complex as they get closer to a cyclotron harmonic. Confluence points that are located off the real axis represent partial wave conversions and in cases where they are not purely imaginary, dissipation occurs as well. Subsequent examination of the local Stokes structure reveals that propagation regions exist between confluence points for some  $n_z$ 's. This indicates that an incoming lower hybrid wave can undergo successive and partial mode conversions with absorption as it propagates into the interior of the plasma.

The global description of the mode conversion process requires a wave equation which is usually derived by an isomorphism between  $k_x$  and  $-i \frac{d}{dx}$  on a polynomial dispersion relation. Such a polynomial is not available if one keeps  $D_E$  in its entire form. However, an approximate second-order dispersion relation valid around each individual confluence point can be readily obtained by Taylor expanding  $D_E$  about a wavenumber  $k_c$ .

$$D_A = (k_x - k_c)^2 - (\delta k_x)^2 = 0 \quad (4)$$

where  $(\delta k_x)^2 = \left. \frac{-2D_E}{\partial^2 D_E / \partial k_x^2} \right|_{k_x=k_c}$  and  $k_c$  satisfies Eq.(3).  $D_A$  couples a lower hybrid wave and a warm plasma wave of equal but opposite group velocities and it becomes an increasingly good approximation to the exact dispersion relation as the group velocity tends to zero ( $\frac{\partial D_A}{\partial k_x} = \pm 2\delta k_x \rightarrow 0$ ), i.e. near a confluence point. The result for a typical case is shown in Fig. 2 where  $D_A$  is evaluated along the real axis ( $\xi = x$ ) and it shows good agreement with  $D_E$  (Fig. 1) near the confluence points. The corresponding differential equation for the wave potential  $\psi$  excluding the fast varying phase  $e^{i \int k_c dx}$  is

$$\frac{d^2 \psi}{dx^2} + (\delta k_x)^2 \psi = 0. \quad (5)$$

Eq.(5) is analytically continued into the complex  $\xi$ -plane to allow for solutions by phase integral method. The confluence points now become the turning points for the potential  $(\delta k_x)^2$ . Treating each turning point separately, the solution to Eq.(5) leads to a wave reflection (conversion) coefficient [9]

$$|\gamma_E|^2 = e^{2i(\sigma - \sigma^*)}$$

where  $\sigma = \int_C \delta k_x d\xi$ . The path C for the phase integral is chosen to follow an anti-Stokes line that emanates from the turning point and terminates when the anti-Stokes line is asymptotic to the real axis [10]. Fig. 4 shows the results for the range of  $n_z$ 's under consideration. The mode conversion efficiency is calculated for each turning point. For  $n_z$ 's between 3.7 and 3.85, there is either no or partial mode conversion at both turning points, thus resulting in a net transmission of the incoming rf power. In the range between 3.9 and 4.5, the mode conversion at the second turning point is total while that at the first increases with  $n_z$ 's up to 4.25. From there to  $n_z = 4.5$  there is practically no conversion at the first turning point.

It has been pointed out by earlier authors that the lower hybrid wave is essentially undamped before mode conversion. By calculating the damping increment from the dispersion curves such as Fig. 1, it is found that there can be considerable absorption of the lower hybrid branch near an ion cyclotron harmonic which is situated before or between confluences depending on the particular  $n_z$  one considers. The present results, therefore, show a substantial departure from previous results in terms of the global energy flow and wave absorption.

## References

- [1] M. Brambilla, *Plasma Physics* **18**, 668 (1976).
- [2] T. H. Stix, *Phys. Rev. Lett.* **15**, 878 (1965).
- [3] P. M. Bellan and M. Porkolab, *Phys. Fluids*, **17**, 1592 (1974).
- [4] H. Kuehl and K. Ko, *Phys. Fluids* **18**, 1816 (1975).
- [5] C. L. Grabbe, *Phys. Fluids* **21**, 1976 (1978).
- [6] V. S. Chan, S. C. Chiu and G. E. Guest, *Phys. Fluids* **23**, 1250 (1980).
- [7] T. Tang, K. Y. Fu and M. W. Farshori, *Plasma Physics* **21**, 127 (1979).
- [8] V. Fuchs, K. Ko and A. Bers, *Phys. Fluids* (to be published).
- [9] J. Heading, *An Introduction to Phase-Integral Methods*, John Wiley and Sons, Inc., New York, 1962.
- [10] R. B. White, *Journal of Computational Physics* **31**, 409 (1979).

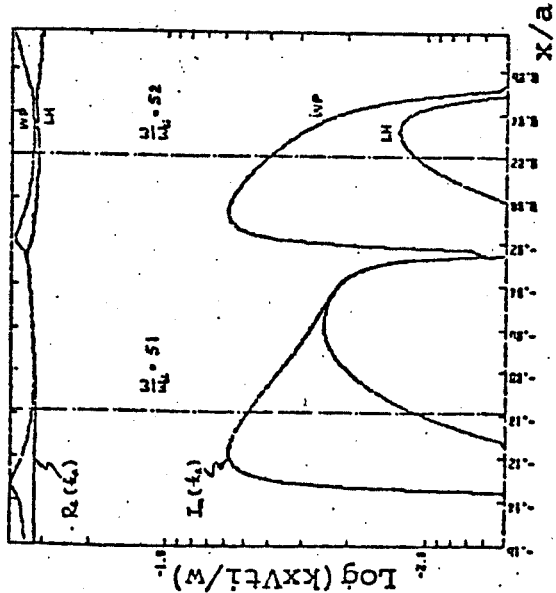


Fig. 1. Dispersion curves from  $D_F$ :  $n_z = 3.9$ ,  $a = 10$  cm; peak values:  $n_0 = 2.75 \times 10^{14} \text{ cm}^{-3}$ ,  $T_e = 1 \text{ keV}$ ,  $T_i = .8 \text{ keV}$ ,  $B_0 = 6.2 \text{ kG}$

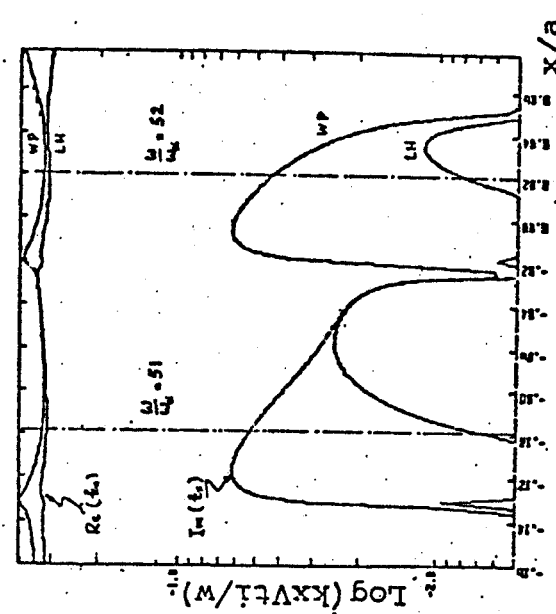


Fig. 2. Dispersion curves from  $D_A$  for similar parameters

$\frac{\omega}{\omega_p}$	$\frac{\omega}{\omega_p}$	$\frac{\omega}{\omega_p}$	$\frac{\omega}{\omega_p}$	$\frac{\omega}{\omega_p}$
0.51	0.51	0.53	0.54	
0.33	0.37	0.41	0.45	
0.375	0.415	0.455	0.495	
0.41	0.445	0.485	0.525	
0.445	0.485	0.525	0.565	
0.485	0.525	0.565	0.605	
0.525	0.565	0.605	0.645	
0.565	0.605	0.645	0.685	
0.605	0.645	0.685	0.725	
0.645	0.685	0.725	0.765	
0.725	0.765	0.805	0.845	
0.805	0.845	0.885	0.925	
0.885	0.925	0.965	1.005	
0.965	1.005	1.045	1.085	
1.045	1.085	1.125	1.165	
1.165	1.205	1.245	1.285	
1.285	1.325	1.365	1.405	
1.405	1.445	1.485	1.525	
1.525	1.565	1.605	1.645	
1.645	1.685	1.725	1.765	
1.765	1.805	1.845	1.885	
1.885	1.925	1.965	2.005	
2.005	2.045	2.085	2.125	
2.125	2.165	2.205	2.245	
2.245	2.285	2.325	2.365	
2.365	2.405	2.445	2.485	
2.485	2.525	2.565	2.605	
2.605	2.645	2.685	2.725	
2.725	2.765	2.805	2.845	
2.845	2.885	2.925	2.965	
2.965	3.005	3.045	3.085	
3.085	3.125	3.165	3.205	
3.205	3.245	3.285	3.325	
3.325	3.365	3.405	3.445	
3.445	3.485	3.525	3.565	
3.565	3.605	3.645	3.685	
3.685	3.725	3.765	3.805	
3.805	3.845	3.885	3.925	
3.925	3.965	4.005	4.045	
4.045	4.085	4.125	4.165	
4.165	4.205	4.245	4.285	
4.285	4.325	4.365	4.405	
4.405	4.445	4.485	4.525	
4.525	4.565	4.605	4.645	
4.645	4.685	4.725	4.765	
4.765	4.805	4.845	4.885	
4.885	4.925	4.965	5.005	
5.005	5.045	5.085	5.125	
5.125	5.165	5.205	5.245	
5.245	5.285	5.325	5.365	
5.365	5.405	5.445	5.485	
5.485	5.525	5.565	5.605	
5.605	5.645	5.685	5.725	
5.725	5.765	5.805	5.845	
5.845	5.885	5.925	5.965	
5.965	6.005	6.045	6.085	
6.085	6.125	6.165	6.205	
6.205	6.245	6.285	6.325	
6.325	6.365	6.405	6.445	
6.445	6.485	6.525	6.565	
6.565	6.605	6.645	6.685	
6.685	6.725	6.765	6.805	
6.805	6.845	6.885	6.925	
6.925	6.965	7.005	7.045	
7.045	7.085	7.125	7.165	
7.165	7.205	7.245	7.285	
7.285	7.325	7.365	7.405	
7.405	7.445	7.485	7.525	
7.525	7.565	7.605	7.645	
7.645	7.685	7.725	7.765	
7.765	7.805	7.845	7.885	
7.885	7.925	7.965	8.005	
8.005	8.045	8.085	8.125	
8.125	8.165	8.205	8.245	
8.245	8.285	8.325	8.365	
8.365	8.405	8.445	8.485	
8.485	8.525	8.565	8.605	
8.605	8.645	8.685	8.725	
8.725	8.765	8.805	8.845	
8.845	8.885	8.925	8.965	
8.965	9.005	9.045	9.085	
9.085	9.125	9.165	9.205	
9.205	9.245	9.285	9.325	
9.325	9.365	9.405	9.445	
9.445	9.485	9.525	9.565	
9.565	9.605	9.645	9.685	
9.685	9.725	9.765	9.805	
9.805	9.845	9.885	9.925	
9.925	9.965	10.005		

Fig. 3. Locations of confluence points in  $\xi$ -plane.

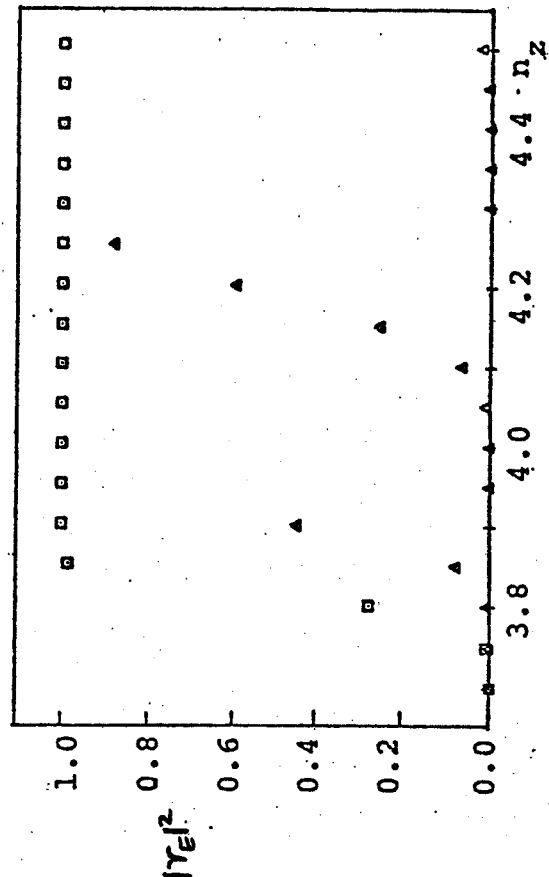


Fig. 4. Mode conversion efficiency vs.  $n_z$ .